

Electrophilic Aldehydes Generated by Sperm Metabolism Activate Mitochondrial Reactive Oxygen Species Generation and Apoptosis by Targeting Succinate Dehydrogenase^{*[5]}

Received for publication, March 26, 2012, and in revised form, July 9, 2012. Published, JBC Papers in Press, July 31, 2012, DOI 10.1074/jbc.M112.366690

R. John Aitken¹, Sara Whiting, Geoffry N. De Iuliis, Samantha McClymont, Lisa A. Mitchell, and Mark A. Baker

From the Priority Research Centre in Reproductive Science, Discipline of Biological Sciences, Faculty of Science and IT, University of Newcastle, University Drive, Callaghan, New South Wales 2308, Australia

Background: The factors responsible for pathological levels of superoxide generation by sperm mitochondria in cases of male infertility are unknown.

Results: Electrophilic aldehydes activate mitochondrial superoxide production by forming adducts with succinate dehydrogenase; nucleophiles counteract this effect and promote sperm survival.

Conclusion: Products of lipid peroxidation activate mitochondrial superoxide generation.

Significance: These findings clarify the causes of oxidative stress in human spermatozoa.

Oxidative stress is a major cause of defective sperm function in cases of male infertility. Such stress is known to be associated with high levels of superoxide production by the sperm mitochondria; however, the causes of this aberrant activity are unknown. Here we show that electrophilic aldehydes such as 4-hydroxynonenal (4HNE) and acrolein, generated as a result of lipid peroxidation, target the mitochondria of human spermatozoa and stimulate mitochondrial superoxide generation in a dose- and time-dependent manner. The activation of mitochondrial electron leakage by 4HNE is shown to involve the disruption of succinate dehydrogenase activity and subsequent activation of an intrinsic apoptotic cascade beginning with a loss of mitochondrial membrane potential and terminating in oxidative DNA adduct formation, DNA strand breakage, and cell death. A tight correlation between spontaneous mitochondrial superoxide generation and 4HNE content ($R^2 = 0.89$) in untreated populations of human spermatozoa emphasized the pathophysiological significance of these findings. The latter also provide a biochemical explanation for the self-perpetuating nature of oxidative stress in the male germ line, with the products of lipid peroxidation stimulating free radical generation by the sperm mitochondria in a positive feedback loop.

Male infertility is a relatively common clinical condition affecting approximately 50% of infertile couples (1). In a vast majority of such patients the infertility is due to a loss of sperm function rather than a lack of sperm numbers (2). One of the major reasons for this loss of functional competence is thought to be oxidative stress (3–6). Spermatozoa are particularly susceptible to this kind of attack because their highly specialized architecture, featuring negligible cytoplasmic space, limits the

availability of cytoplasmic enzymes, such as superoxide dismutase or glutathione peroxidase, that protect most cell types from exposure to reactive oxygen species (ROS)² (7). Second, these cells offer an abundance of substrates for free radical attack including polyunsaturated fatty acids and DNA, both of which become oxidatively damaged in the spermatozoa of male infertility patients (8–10). Furthermore, once oxidative damage has been sustained, these terminally differentiated cells have very limited capacity for self-repair (11). In addition, spermatozoa are professional generators of ROS, including hydrogen peroxide and superoxide anion (11). In fact, the cellular production of ROS was first demonstrated in bovine spermatozoa in 1946 (12), predating the discovery of this activity in leukocytes by more than a decade.

The ROS generated by spermatozoa are a two-edged sword. On the one hand, these molecules serve an important physiological function by driving spermatozoa into a physiological state known as “capacitation,” as a result of which they gain the ability to fertilize the oocyte (13–15). On the other, ROS can rapidly overwhelm the limited antioxidant defenses offered by spermatozoa to induce a state of oxidative stress. This results in high levels of DNA damage in the spermatozoa of such patients, the incidence of which is significantly correlated with miscarriage or, if the pregnancy carries to term, impaired health in the offspring (9, 10, 16). At higher levels of oxidative stress, the peroxidative damage to the sperm plasma membrane disrupts various aspects of sperm function, resulting in long term infertility (5).

The source of the ROS responsible for disrupting the functionality of human spermatozoa is thought to involve the mitochondria located in the proximal part of the flagellum in a sub-

^{*} This work was supported by National Health and Medical Research Council Program Grant 494802 (to R. J. A.).

^[5] This article contains supplemental Methods and Figs. 1–4.

¹ To whom correspondence should be addressed: Discipline of Biological Sciences, University of Newcastle, Callaghan, NSW 2308, Australia. Tel.: 61-2-4921-6143; Fax: 61-2-4921-6308; E-mail: john.aitken@newcastle.edu.au.

This is an Open Access article under the CC BY license.

² The abbreviations used are: ROS, reactive oxygen species; BP, bromopyruvate; BWW, Biggers, Whitten, and Whittingham medium; DHE, dihydroethidium; DPI, diphenylene iodonium; FLICA, fluorochrome-labeled inhibitor of caspase activity; 4HNE, 4-hydroxynonenal; IPG, immobilized pH gradient; MICA, 5-methoxyindole-2-carboxylic acid; MSR, MitoSOXTM Red; NEM, N-ethylmaleimide; PLSD, protected least significant difference; SDH, succinate dehydrogenase; SDHA, 72-kDa catalytic subunit of SDH complex II of the mitochondrial electron transport chain.

cellular domain known as the midpiece (17). Mitochondrial ROS production is significantly elevated in poor quality spermatozoa and exhibits a negative correlation with sperm movement (18). Moreover, such impaired motility can be recapitulated by artificially driving ROS production by the sperm mitochondria and reversed by the concomitant presence of an antioxidant in the form of α -tocopherol (18). The factors responsible for inducing ROS generation by sperm mitochondria are now the object of intense investigation. In this study we show that this activity can be elicited by a wide variety of electrophiles including those generated naturally during the process of lipid peroxidation. Furthermore, our study emphasizes the importance of succinate dehydrogenase as a target for 4-hydroxynonenal (4HNE) in activating mitochondrial ROS production. These data emphasize the self-perpetuating nature of oxidative stress in the male germ line and provide a biochemical basis for oxidatively induced ROS generation, which is a characteristic feature of these cells (19).

EXPERIMENTAL PROCEDURES

Reagents and Solutions—All chemicals and reagents were obtained from Sigma-Aldrich unless otherwise stated, and all fluorescent probes were purchased from Molecular Probes. Isotonic Percoll was prepared by supplementing 90 ml of this density gradient centrifugation medium with 10 ml of $10 \times$ Ham's F-10 medium, 370 μ l of a 60% sodium DL-lactate (w/w) syrup, and 3 mg of sodium pyruvate. For all sperm incubations the medium employed was Biggers, Whitten, and Whittingham (BWW) medium containing 1 mg/ml polyvinyl alcohol, 5 units/ml penicillin, and 5 mg/ml streptomycin (20). BWW was prepared fresh daily and, following adjustment of the osmolarity to 290–310 mOsm/kg, was maintained at 37 °C in an atmosphere of 5% CO₂ in air.

Preparation of Human Spermatozoa—Human semen samples were obtained from University of Newcastle donors using protocols that have been given with Institutional and State Government ethical approval. All samples were donated following 48 h abstinence and provided to laboratory staff within 1 h of donation. After allowing at least 30 min for liquefaction to occur, the spermatozoa were fractionated on a discontinuous two-step Percoll gradient (90%/45%), as described previously (21).

Flow Cytometry Measurements—Flow cytometry was performed using a FACSCalibur flow cytometer (BD Biosciences) with a 488-nm argon ion laser. Emission measurements were made using 530/30 band pass (green/FL-1), 585/42 band pass (red/FL-2), and >670 long pass (far red/FL-3) filters. Forward scatter and side scatter measurements were taken to generate a scatter plot, which was used to gate for sperm cells only, excluding any larger contaminating cells. All data were acquired and analyzed using CellQuest Pro software (BD Biosciences), with a total of 10,000 events collected per sample. Cellular and mitochondrial ROS generation were measured with dihydroethidium (DHE) and MitoSOXTM Red (MSR), respectively, in the presence of SYTOX Green to assess cell viability (18, 22). Only results for viable cells are reported. Mitochondrial membrane potential was assessed with JC1 in combination with propidium iodide, using carbonyl cyanide *m*-chlorophenylhydra-

zone at a final concentration of 10 μ M to create a negative control (22), susceptibility to lipid peroxidation with BODIPY C₁₁ (18), caspase activation with fluorochrome-labeled inhibitor of caspase activity (FLICA) (22), phosphatidylserine externalization with annexin V-FITC and propidium iodide (22), oxidative DNA damage with the OxyDNA Assay (Calbiochem) in combination with LIVE/DEAD fixable dead cell stain (Molecular Probes) (22), DNA strand breakage with a modified TUNEL assay (23), and 4HNE with an anti-4HNE antibody (Jomar Diagnostics). For the latter spermatozoa were suspended in 49 μ l of BWW, and 1 μ l of anti-4HNE antiserum was added for 30 min at 37 °C. Cells were spun down at $650 \times g$ for 5 min and washed twice with BWW. They were then resuspended in 99 μ l of BWW, and 1 μ l of secondary antibody (Alexa Fluor 488 goat anti-rabbit IgG) was added for 10 min at 37 °C. Cells were centrifuged again, washed twice with BWW, and resuspended in 400 μ l of BWW for analysis by flow cytometry.

Chemiluminescence—The impact of the flavoprotein inhibitor, diphenylene iodonium (DPI), on the ability of 4HNE to trigger a ROS response in human spermatozoa was determined by chemiluminescence using luminol/peroxidase as the probe, as previously described (21).

Gel Electrophoresis and Western Blotting—For conventional one-dimensional SDS-PAGE and Western blotting procedures, sperm proteins were extracted with sodium dodecyl sulfate (SDS) extraction buffer (2% SDS, 10% sucrose in 0.1875 M Tris, pH 6.8) containing a protease inhibitor mixture (Roche Applied Science) at 100 °C for 5 min. The spermatozoa were then subjected to SDS-PAGE and Western blotting procedures performed as described (22). The primary antibodies used in these studies were anti-4HNE (Jomar Diagnostics) at 1:500 and an anti-SDHA antibody (complex II subunit 70-kDa Fp mAb (Sapphire Biosciences)). HRP-labeled goat anti-rabbit (1:1000 in 1% skim milk for 1 h at room temperature) and goat anti-mouse (1:1000 with 1% BSA for 1 h at room temperature) were used as secondary antibodies, respectively.

For two-dimensional electrophoresis and Western blotting, protein was extracted from spermatozoa, following incubation for 2 h with or without 250 μ M 4HNE, using 7 M urea, 2 M thiourea, and 4% w/v CHAPS for 1 h under rotation at 4 °C. Following centrifugation, the protein content of the supernatant was determined using a two-dimensional Quant-kit (GE Healthcare), and the proteins were precipitated using a modified methanol:chloroform procedure as described elsewhere (24). Immobilized pH gradient (IPG) strips with a pH range of 4–7 were chosen to separate the proteins. Following protein separation, the IPG strips were placed in equilibration buffer (50 mM Tris, 0.5% SDS, 4.7 M glycerol, 6.3 M urea, and dH₂O) with 32 mM DTT for 10 min, followed by 243 mM iodoacetamide for 10 min. The IPG strips were sealed with agar on a 10% SDS gel with the plus end of the strip being next to the protein markers. The gel was run at 150 V until the dye front ran off the gel. Proteins were then semitransferred to a nitrocellulose membrane using 350 mA for 10 min. The gels were placed in 10% methanol and 5% acetic acid until ready for silver staining. The membranes were blocked with 5% skim milk for 1 h at room temperature, washed with TBST (Tris-buffered saline containing 0.01% Tween 20), and incubated overnight in pri-

mary antibody (anti-4HNE) at 1:500 with 1% BSA at 4 °C. The primary antibody was removed with TBST, and secondary antibody (goat anti-rabbit HRP) was added at 1:1000 with 1% skim milk for 1 h at room temperature. Proteins were ultimately visualized using an enhanced chemiluminescence kit (GE Healthcare) according to the manufacturer's instructions.

Proteomics—Proteins that were shown to bind 4HNE on the two-dimensional Western blot were located on the silver-stained gel and cut out for identification. The gel plugs were placed into a 96-well plate and destained using 12 mM potassium ferricyanide and 32 mM sodium thiosulfate. Gel plugs were washed with dH₂O until clear, and 150 μ l of plug washing solution (10 ml methanol, 0.0395 g of ammonium bicarbonate, made up to 20 ml with dH₂O) was added and mixed. The plugs were then washed several times over a period of 30 min at room temperature and incubated for 1 h at 37 °C for dehydration; 2 μ l of trypsin (10 μ g/ml in 25 mM ammonium bicarbonate) was then added to each gel plug and incubated overnight at room temperature with a seal over the plate. The trypsinized samples were subsequently analyzed by MALDI TOF/TOF mass spectrometry.

Succinate Dehydrogenase (SDH) Immunoprecipitation—For the immunoprecipitation studies, the anti-SDHA antibody was attached to A/G PLUS-agarose beads (Thermo Fisher) according to the manufacturer's instructions. The beads were then resuspended in 250 μ g of sperm protein lysate, prepared by extracting human spermatozoa with 10 mM CHAPS for 1 h at 4 °C, and subjected to constant rotation for 15 h at 4 °C. The beads were then washed three times with PBS before being boiled for 5 min with SDS loading buffer (0.2% w/v SDS, 50% v/v 0.375 M Tris, 10% w/v sucrose, 4% v/v β -mercaptoethanol, and 0.001% bromophenol blue). The proteins were subsequently separated on a 4–20% gradient gel along with a range of controls including SDS extracts of beads alone, antibody alone, antibody-loaded beads not incubated with lysate, and lysate pre-cleared with beads not loaded with antibody. The proteins were subsequently transferred to a nitrocellulose membrane (GE Healthcare) using 350 mA for 60 min. The membranes were subsequently washed in TBST for 10 min, blocked with 3% BSA for 1 h at room temperature, and then probed with anti-4HNE antiserum (1:500 with 1% skim milk overnight at 4 °C) followed by secondary antibody (goat anti-rabbit HRP; 1:1000 in 1% skim milk for 1 h at room temperature). The blot was then stripped and reprobed with anti-SDHA antibody (1:1000 with 1% BSA overnight at 4 °C), followed by the corresponding secondary antibody (goat anti-mouse HRP; 1:1000 with 1% BSA for 1 h at room temperature). An irrelevant monoclonal antibody, anti-Rho A (Santa Cruz Biotechnology), was employed as a control for this secondary. Proteins were visualized using enhanced chemiluminescence (GE Healthcare).

SDH and Cytochrome Oxidase Activities—SDH and cytochrome oxidase activities were determined by measuring the reduction of 2,6-dichloroindophenol and the oxidation of reduced cytochrome *c* as described in supplemental Methods.

Cytochrome *c* Release—A Western blot procedure was used to detect cytochrome *c* released into the extracellular space following permeabilization of the spermatozoa with filipin. This compound has previously been shown to permeabilize the

plasma membrane of spermatozoa while leaving the mitochondria in an intact functional state (25). For the assay, spermatozoa were treated with 4HNE (25–200 μ M) for 3 h at 37 °C. They were then pelleted and resuspended in 60 μ l of BWW containing 25 μ M filipin III for 2 min at room temperature. The spermatozoa were pelleted again and the supernatant probed for cytochrome *c* using a Western blot procedure (22).

Electrophilicity Calculations—Both Hartree-Fock and density functional theory calculations were performed on geometry optimized models of each compound (26). The 6–31G* basis set was used for both methods, and the B3-LYP exchange correlation potential was implemented for the density functional theory calculations. The energies for both the highest occupied molecular orbital (HOMO) and the lowest unoccupied molecular orbital (LUMO) were then obtained from each calculation method (Hartree-Fock and density functional theory). The electrophilicity index (ω) was calculated from the HOMO and LUMO energies for each compound as follows: hardness: $\eta = (\epsilon\text{LUMO} - \text{HOMO})$; chemical potential: $\mu = -(\epsilon\text{HOMO} + \epsilon\text{LUMO})/2$; electrophilicity index: $\omega = \mu^2/(2\eta)$.

The alkylating power of a range of electrophiles was also determined using the kinetic glutathione assay described by Bohme *et al.* (27) as detailed in supplemental Methods.

Statistics—All experiments were repeated at least three times on independent samples, and the results analyzed by ANOVA using the SuperANOVA program (Abacus Concepts) on a MacIntosh G4 computer; post hoc comparison of group means was by Fisher's PLSD (protected least significant difference). Paired comparisons were conducted using a paired *t* test. Differences with a *p* value of < 0.05% were regarded as significant.

RESULTS

Electrophiles, Including Naturally Occurring Cytotoxic Aldehydes, Induce Mitochondrial ROS Generation in Human Spermatozoa—This study was initiated by the discovery that a quinone (1,4-benzoquinone), already known for its ability to induce the rapid immobilization of human spermatozoa (28), was capable of inducing a highly significant (*p* < 0.001) dose-dependent increase in mitochondrial ROS generation that peaked at 12.5 μ M and then declined at higher doses (Fig. 1A). These actions were not unique to benzoquinone because other electrophiles such as iodoacetamide (Fig. 1B), *N*-ethylmaleimide (NEM; Fig. 1C), and ethyl vinyl ketone (Fig. 1D) had similar activating effects on mitochondrial ROS, although the optimal concentration for inducing this activity varied significantly between compounds (12.5 μ M (benzoquinone), 50 μ M (NEM), 400 μ M (ethyl vinyl ketone), and 800 μ M (iodoacetamide)). All of these compounds also induced a dramatic loss of motility prior to any change in vitality at doses that exceeded those needed to generate mitochondrial ROS (Fig. 1, A–D). The selectivity of these electrophilic effects was emphasized by the fact that certain electrophiles such as acrylamide possessed no detectable capacity to stimulate mitochondrial ROS or suppress sperm movement (Fig. 1E).

These primary observations were followed up by assessments of naturally generated electrophiles for their ability to activate mitochondrial ROS generation in human spermatozoa. The focus of this analysis was on the aldehydes, acrolein, and

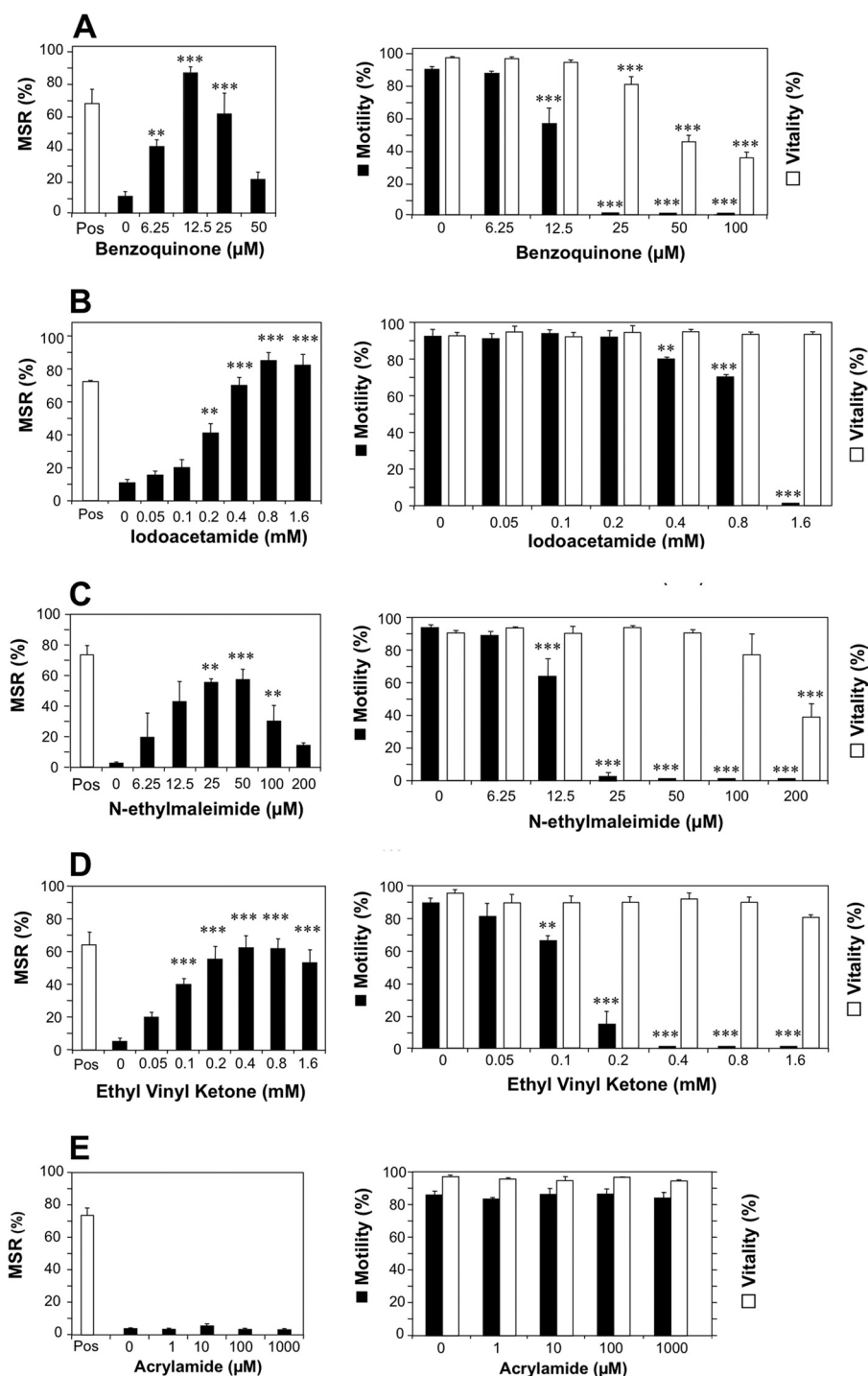


FIGURE 1. Impacts of synthetic electrophiles on the generation of mitochondrial ROS, motility, and vitality of human spermatozoa. Left panels depict flow cytometry analyses, revealing the dose-dependent impact of electrophiles on the generation of mitochondrial ROS by human spermatozoa. Mitochondrial ROS in live cells was measured with MSR in conjunction with SYTOX Green following a 2-h exposure. Pos, positive control incubations involving exposure to arachidonic acid ($5 \mu\text{M}$) for 5 min at 37°C . Right panels demonstrate the impact of the same electrophiles on sperm motility (filled bars) and vitality as assessed by SYTOX Green (open bars). The electrophiles examined comprised benzoquinone (A), iodoacetamide (B), NEM (C), ethyl vinyl ketone (D), and acrylamide (E). All of the electrophiles tested except acrylamide demonstrated a capacity to stimulate mitochondrial ROS generation and suppress motility in live cells. Data were analyzed by ANOVA, and values are presented as means \pm S.E. (error bars); ***, $p < 0.001$; **, $p < 0.01$ for differences with negative control by Fisher's PLSD. All analyses were replicated on three independent semen samples except benzoquinone data, which were replicated on nine individual samples.

4HNE, which are generated as a result of the breakdown of lipid peroxides. With both of these electrophiles, a highly significant ($p < 0.001$) dose-dependent induction of mitochondrial ROS was observed, peaking at $200 \mu\text{M}$ and then declining (Fig. 2, A and B). Just as we observed with most of the synthetic electro-

philes, a significant loss of motility ($p < 0.001$) was observed with acrolein and 4HNE at doses where the viability of the cells had not yet been compromised (Fig. 2, A and B). To be certain of the biological significance of these observations these experiments were repeated with lower doses of 4HNE (6.25 – $50 \mu\text{M}$)

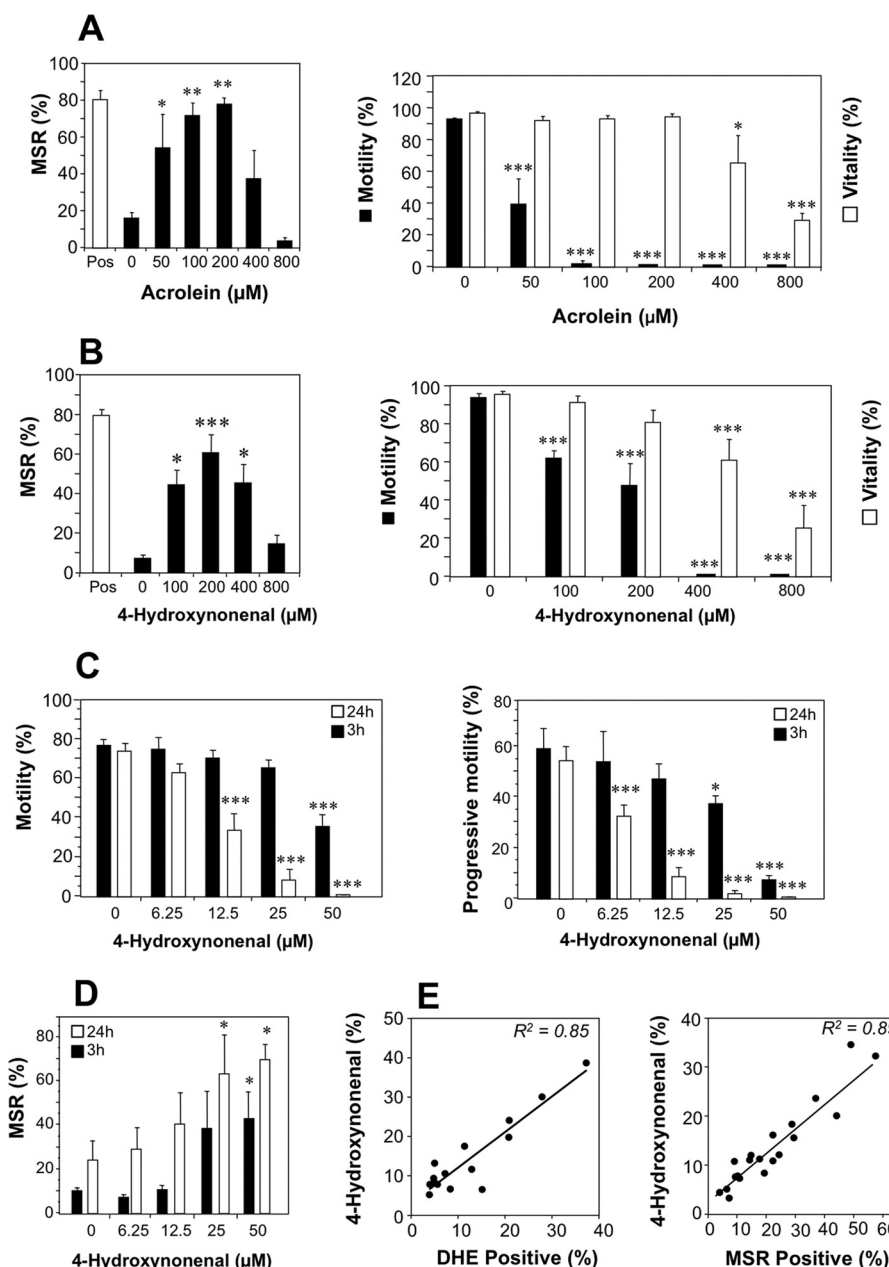


FIGURE 2. The naturally occurring lipid aldehydes, 4HNE and acrolein, induce mitochondrial ROS generation in human spermatozoa. A, flow cytometry of the generation of mitochondrial ROS, motility, and vitality of spermatozoa exposed to the naturally occurring electrophile, acrolein, was analyzed. The exposure conditions (2 h at 37 °C) and measurements were identical to those described in Fig. 1. Acrolein stimulated a dose-dependent increase in mitochondrial ROS (MSR), that peaked at 200 μM , coupled with a significant loss of sperm motility (filled bars) at doses that preceded a loss of cell viability (open bars). B, parallel data for 4HNE are presented. C, to confirm the physiological significance of these electrophilic effects, motility, and progressive motility were also examined with lower doses of 4HNE (6.25–50 μM) after 3 h (filled bars) and 24 h (open bars) of exposure, and highly significant inhibitory effects observed that were both time- ($p < 0.001$) and dose- ($p < 0.001$) dependent by ANOVA. D, low doses of 4HNE were also found to induce time- ($p = 0.011$) and dose- ($p = 0.003$) dependent increases in the percentage of live cells producing mitochondrial ROS, when assessed after 3 h (filled bars) and 24 h (open bars) of exposure. E, physiological significance was also emphasized by the highly significant correlations ($p < 0.001$) observed between the 4HNE content of human spermatozoa and their spontaneous capacity for generating ROS whether determined by the oxidation of DHE as a measure of overall cellular ROS generation ($R^2 = 0.85$, left) or MSR, focusing on the mitochondrial contribution (right, $R^2 = 0.89$). Data analyzed by ANOVA and values are presented as means \pm S.E. (error bars); ***, $p < 0.001$; **, $p < 0.01$; *, $p < 0.05$ for differences with vehicle control by Fisher's PLSD. Analyses were based on three independent semen samples for acrolein and four independent samples for 4HNE.

that are well within the physiological range. These studies revealed both time- ($p < 0.001$) and dose-dependent ($p < 0.001$) decreases in motility and progressive motility on exposure to 4HNE (Fig. 2C). These low doses of 4HNE also stimulated high significant increases in the generation of mitochondrial ROS by live cells that were both time- ($p = 0.011$) and dose-dependent ($p < 0.003$) (Fig. 2D).

The pathophysiological importance of this relationship between cytotoxic aldehyde exposure and the generation of mitochondrial ROS was indicated by the existence of highly significant ($p < 0.001$) relationships between the spontaneous levels of 4HNE expression by human spermatozoa and their overall level of cellular ROS generation as reflected by DHE oxidation (Fig. 2E, left panel; $R^2 = 0.85$). Furthermore, an even

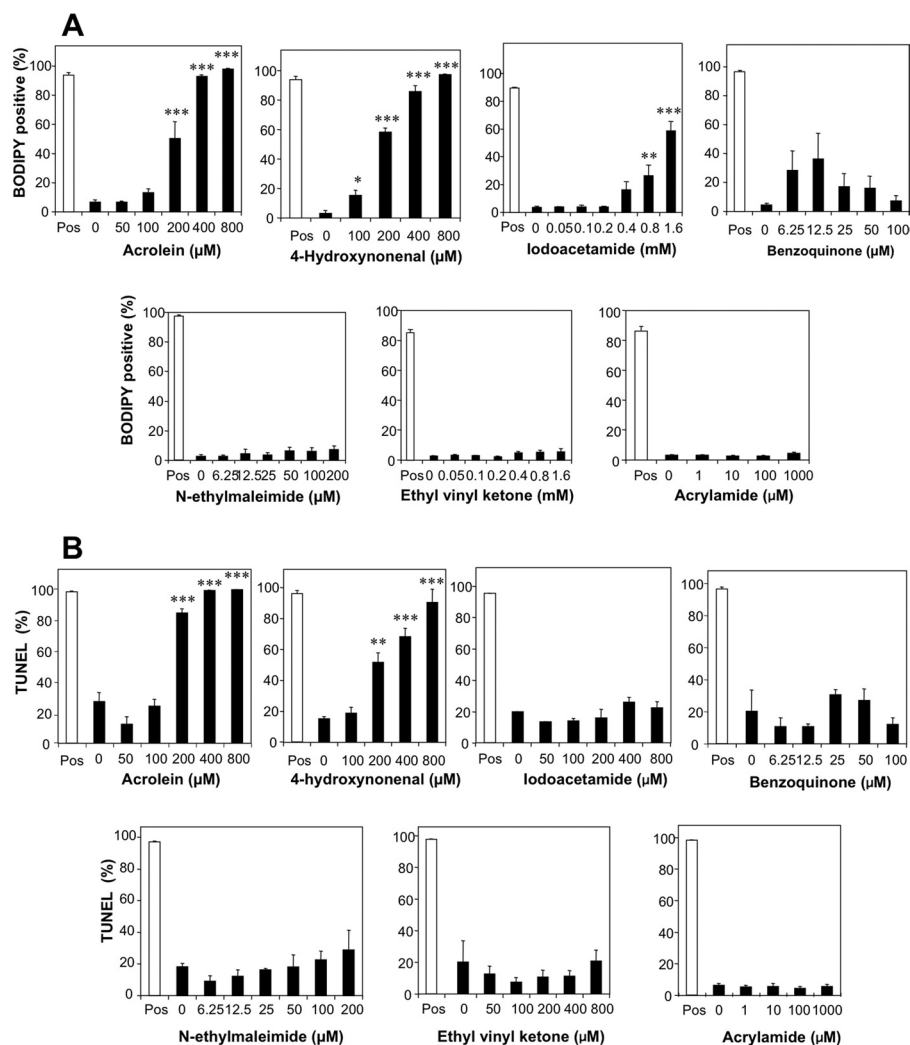


FIGURE 3. Impact of electrophiles on levels of lipid peroxidation and DNA fragmentation observed in human spermatozoa. *A*, exposure of human spermatozoa to the lipid aldehydes, acrolein and 4HNE, triggered a highly significant ($p < 0.001$) dose-dependent increase in lipid peroxidation, which was not observed with other electrophiles, with the exception of high doses of iodoacetamide. Percoll-purified spermatozoa were loaded with BODIPY C_{11} for 30 min at 37 °C and then incubated for 2 h at 37 °C prior to analysis by flow cytometry. The positive control (*Pos*, open bars) was treated with 80 μ M ferrous sulfate. *B*, the ability of acrolein and 4HNE to trigger a rapid increase in lipid peroxidation was reflected in their unique ability to induce high levels of DNA fragmentation, suggesting that these compounds are particularly effective inducers of the intrinsic apoptotic cascade. Samples were incubated for 24 h at 37 °C before being processed for the TUNEL assay, adapted for the compacted nature of sperm chromatin as described under "Experimental Procedures." Positive control (*Pos*, open bars) incubations were treated with DNase for 1 h at 37 °C. Data were analyzed by ANOVA, and values are presented as means \pm S.E. (error bars); ***, $p < 0.001$; **, $p < 0.01$ for differences with vehicle control by Fisher's PLSD. Analyses were based on three independent semen samples.

more powerful correlation was observed when the analysis focused on ROS generation by the mitochondria (Fig. 2*E*, right panel; $R^2 = 0.89$).

Direct comparison of all the above electrophiles at a single dose (100 μ M) for their relative ability to trigger mitochondrial ROS revealed a spectrum of activity with acrolein, 4HNE, ethyl vinyl ketone, and NEM as the most active compounds (supplemental Fig. 1). Calculation of the electron reduction potentials of the compounds tested suggested that the ability of these chemicals to trigger mitochondrial ROS production was significantly correlated with their electrophilicity as measured experimentally using glutathione as the nucleophile ($R^2 = 0.63$), but not when assessed theoretically via Hartree-Fock and density functional theory calculations (supplemental Fig. 2, *A* and *B*).

The Naturally Occurring Electrophilic Aldehydes, 4HNE and Acrolein, Are Powerful Inducers of Apoptosis in Sperm, Inducing

Lipid Peroxidation and DNA Damage—Analysis of the ability of various electrophiles to induce lipid peroxidation in human spermatozoa using BODIPY C_{11} as the probe, revealed that both 4HNE ($p < 0.001$) and acrolein ($p < 0.001$) were particularly active in this regard (Fig. 3*A*). Of the other electrophiles tested, only high doses of iodoacetamide succeeded in inducing an increase in lipid peroxidation (Fig. 3*A*). The remaining electrophiles such as ethyl vinyl ketone, benzoquinone, and NEM failed to induce significant lipid peroxide formation over the 2-h time course of these experiments. Similarly, a 24-h exposure to 4HNE and acrolein was sufficient to induce a dose-dependent increase in DNA fragmentation as measured in the TUNEL assay, whereas none of the other electrophiles examined was capable of damaging the tightly compacted nuclear genome of spermatozoa within this time frame (Fig. 3*B*).

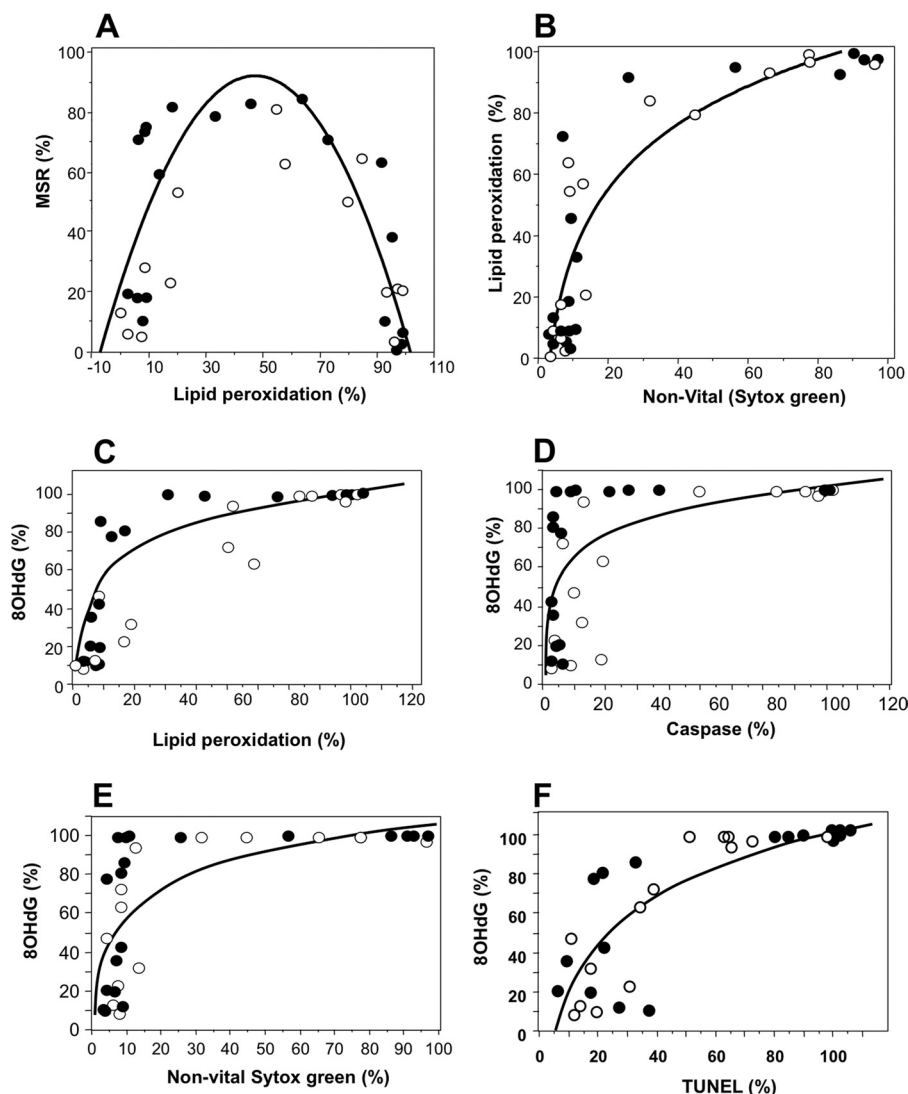


FIGURE 4. Relationship between mitochondrial ROS generation triggered by lipid aldehydes, oxidative stress, and apoptosis in human spermatozoa. A, exposure of human spermatozoa to the lipid aldehydes, acrolein and 4HNE, induced a rapid rise in mitochondrial ROS generation and lipid peroxidation that peaked and then fell as $>50\%$ of the sperm populations became peroxidation-positive. Mitochondrial ROS generation and lipid peroxidation were measured by flow cytometry after a 2-h exposure at 37°C , using MSR and BODIPY C_{11} as probes ($p < 0.001$; $y = 14.387 + 2.862x - 0.029x^2$; $R^2 = 0.587$). Open circles, 4HNE; filled circles, acrolein. B, the lipid peroxidation triggered by acrolein and 4HNE (BODIPY C_{11}) resulted in a sudden increase in cell death detected with SYTOX Green, once approximately 70% of the cell population had become peroxidation (4HNE)-positive ($p < 0.001$; $y = 36.379 + 70.396\log x$; $R^2 = 0.806$). Open circles, 4HNE; filled circles, acrolein. C, the lipid peroxidation triggered by acrolein and 4HNE was also associated with a rise in oxidative DNA damage, measured by flow cytometry using 8OHdG formation as the criterion ($p < 0.001$; $y = 1.835 + 20.552\ln(x)$; $R^2 = 0.709$). Open circles, 4HNE; filled circles, acrolein. D, once approximately 80% of the cells became positive for 8OHdG there was a sudden increase in the percentage of caspase-positive cells, measured using the FLICA probe in conjunction with flow cytometry ($p < 0.001$; $y = 23.078 + 16.982\ln(x)$; $R^2 = 0.405$). Open circles, 4HNE; filled circles, acrolein. Data were taken from the dose-response experiments employing a 50–800 μM concentration of each electrophile. E, at high levels of 8OHdG formation, there was a sudden loss of cell viability, measured using SYTOX Green ($p < 0.001$; $y = 6.26 + 22.333\ln(x)$; $R^2 = 0.504$). Open circles, 4HNE; filled circles, acrolein. F, the increase in 8OHdG formation was also associated with a sudden increase in DNA fragmentation as reflected in the TUNEL assay ($p < 0.001$; $y = -60.959 + 35.143\ln(x)$; $R^2 = 0.671$). Open circles, 4HNE; filled circles, acrolein.

When the data from these dose-response studies were analyzed further, the particularly powerful induction of lipid peroxidation with acrolein and 4HNE was found to exhibit a near perfect parabolic relationship with mitochondrial ROS generation (Fig. 4A). This relationship reflected the fact that mitochondrial ROS generation is an active metabolic process that can only be exhibited by live cells. Scattergram plots of lipid peroxidation and vitality revealed that exposure to 4HNE and acrolein induced a rapid rise in lipid peroxide levels up the point where approximately 70% of the cell population was positive, without any major changes in cell viability (Fig. 4B). However,

as the level of peroxidative damage proceeded beyond this point, cell vitality declined rapidly and with it, the ability of the spermatozoa to generate mitochondrial ROS (Fig. 4, A and B).

The induction of lipid peroxidation with acrolein and 4HNE was also accompanied by a rise in oxidative DNA damage, monitored as 8OHdG (Fig. 4C) which was followed by all of the hallmarks of apoptosis including caspase activation (Fig. 4D) cell death (Fig. 4E), and DNA fragmentation (Fig. 4F). In light of these relationships between oxidative stress and DNA damage, highly significant correlations were observed between lipid peroxidation and TUNEL, which was linear in the case of 4HNE

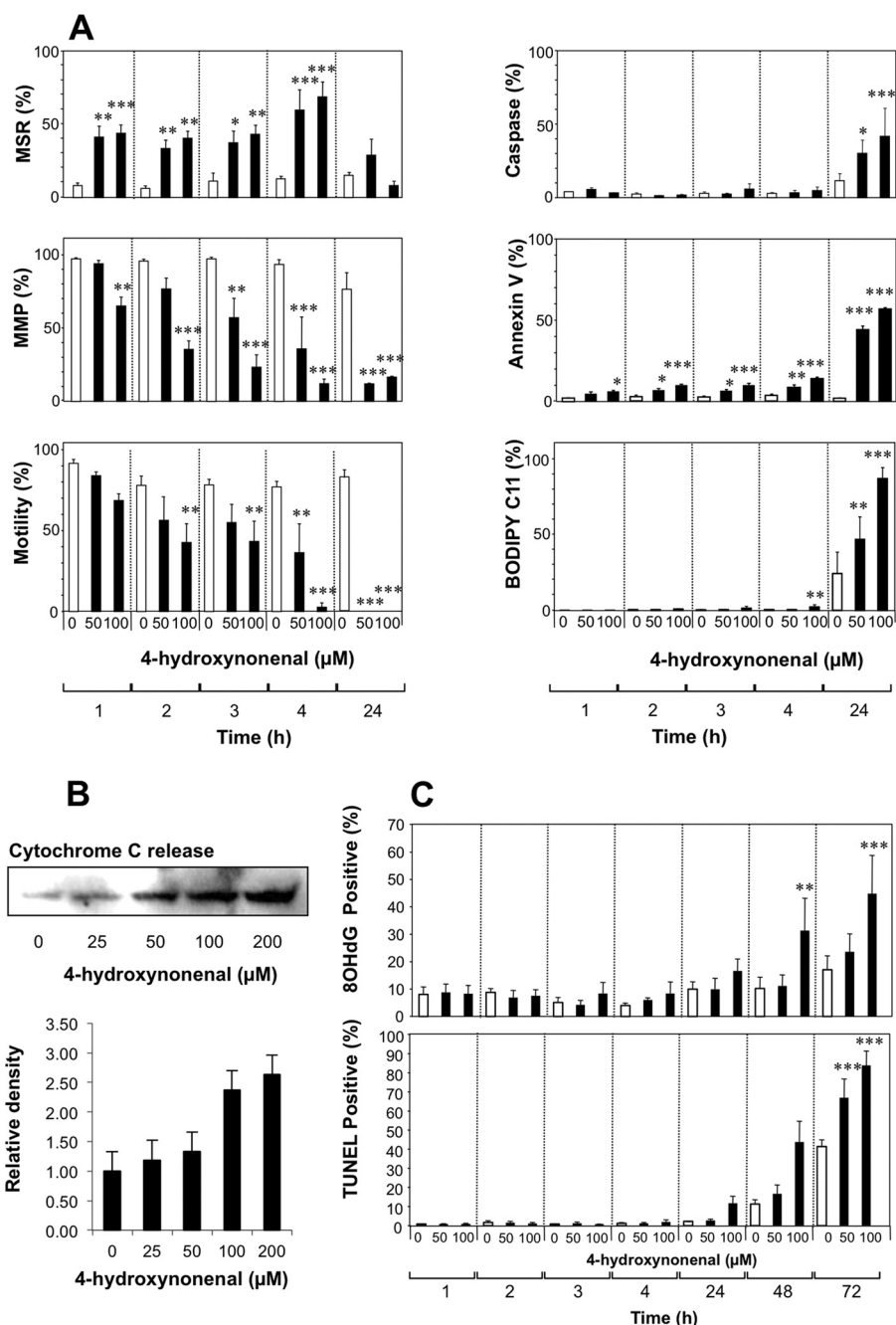


FIGURE 5. Time course analysis of the cascade of events set in motion when human spermatozoa are exposed to lipid aldehydes. A, exposure to physiological amounts of 4HNE (50 and 100 μM) for up to 24 h at 37 °C resulted in a rapid stimulation of mitochondrial ROS (MSR), that was maximal after 4 h but then declined over the ensuing 20 h. Significant changes in mitochondrial membrane potential (MMP) were also evident within 3 h of 4HNE exposure and declined to minimal levels by 24 h. The inhibition of sperm motility with 4HNE paralleled mitochondrial membrane potential disruption, being significant at both 50 and 100 μM within 4 h of 4HNE exposure and reaching undetectable levels within 24 h. The remaining aspects of apoptosis assessed in this study including caspase activation, annexin V binding to the surface of viable cells, and lipid peroxidation, were minimally affected during the first 4 h of 4HNE exposure but then became maximal at 24 h. Open bars, control incubations; filled bars, 4HNE-treated. B, cytochrome c release from the mitochondria was elevated in a dose-dependent manner after a 3-h incubation with 4HNE (25–200 μM). Upper panel shows Western blots whereas lower panel presents densitometric scans from three independent experiments. C, under the conditions of this experiment, DNA damage, whether measured in terms of 8OHdG formation or TUNEL positivity, did not start to increase dramatically until the cells had been exposed to 4HNE for 48–72 h and thus represents an extremely late event in the apoptotic pathway. Open bars, control incubations; filled bars, 4HNE-treated. Data analyzed by ANOVA and values are presented as means \pm S.E. (error bars); ***, $p < 0.001$; **, $p < 0.01$; *, $p < 0.05$ for differences with vehicle control by Fisher's PLSD. Analyses were based on three independent semen samples.

($R^2 = 0.807$; $p < 0.001$) but exponential in the case of the more powerful acrolein ($R^2 = 0.807$; $p < 0.0001$; supplemental Fig. 3, A and B).

Apoptosis and DNA Damage Induced by 4HNE—Using physiological concentrations (50 and 100 μM) of 4HNE (29), we then

mapped the time course of these apoptotic responses to this electrophile. Within 1 h of exposure to 4HNE, mitochondrial ROS was significantly activated at both doses examined (Fig. 5A). Over the next 3 h mitochondrial membrane potential declined in a dose-dependent manner, and motility was signif-

icantly impaired. In addition, an analysis of cytochrome *c* release at this early time point revealed a clear dose-dependent increase in the discharge of this apoptotic marker from the mitochondria in response to 25–200 μM 4HNE (Fig. 5B). However, no major changes in vitality, caspase activation, annexin V binding or lipid peroxidation were observed at this early time point (Fig. 5A). After 24 h, however, apoptosis was well advanced, and all of these markers were significantly changed in a dose-dependent manner (Fig. 5A). Subsequent to the appearance of these apoptotic changes, the cells exhibited increases in 8OHdG formation and DNA strand breakage that first became apparent after 48 h and were highly significant by 72 h after exposure (Fig. 5C). Exposure to electrophilic aldehydes that are generated as a consequence of sperm metabolism therefore activates a prolonged apoptotic cascade in human spermatozoa that is initiated by an increase in mitochondrial ROS generation and culminates in oxidative DNA damage, DNA strand breakage, and death. Although nucleases are activated during this process, the unique compartmentalized nature of human spermatozoa means that these effectors of DNA fragmentation do not gain access to sperm chromatin (22). As a result, the only mechanism by which sperm DNA can become damaged during apoptosis involves an oxidative attack by ROS generated by the sperm mitochondria (22).

Elucidation of Mechanisms by Which Electrophiles Activate Mitochondrial ROS Generation and Apoptosis in Human Spermatozoa—To elucidate the mechanism by which electrophiles such as 4HNE might activate ROS generation by human spermatozoa, we began by examining the subcellular sites of 4HNE adduction in spermatozoa using immunofluorescence microscopy. These studies demonstrated that the major sites for 4HNE adduction in human spermatozoa are the mitochondria located in the sperm midpiece (Fig. 6A). Western blot analyses subsequently demonstrated that 4HNE complexed with a number of major proteins in human spermatozoa, some of which were definitively identified by mass spectrometry including HSP70, dihydrolipoyl dehydrogenase, tektin 3, α - and β -enolase, and ATP synthase subunit β (Fig. 6B). From this list of alkylated proteins we selected two for further investigation as potential mediators of mitochondrial ROS generation in human spermatozoa.

The first of these candidates was the β -subunit of the mitochondrial ATP synthase. Using oligomycin to block ATPase activity, we demonstrated that neither high doses of this compound up to 800 μM nor prolonged exposure to this reagent for 24 h had any significant effect on mitochondrial ROS generation by human spermatozoa (data not shown).

The second adducted target assessed was dihydrolipoyl dehydrogenase, the E3 component of the pyruvate dehydrogenase complex. To examine the role of this complex in mitochondrial ROS generation we determined the impact of 5-methoxyindole-2-carboxylic acid (MICA), a recognized inhibitor of this enzyme, which has also been shown to disrupt the functionality of hamster spermatozoa *in vitro* (31). At exactly the same dose as employed in the hamster study (5 mM) MICA had no detectable impact on mitochondrial ROS generation (Fig. 6C). In light of this negative result, another inhibitor of the pyruvate dehydrogenase complex, bromopyruvate (BP), was assessed for its

impact on mitochondrial free radical generation (31). A low dose of this reagent (50 μM) had a profound ($p < 0.001$) stimulatory effect on mitochondrial ROS generation (Fig. 6C) stimulating approximately 60% of the cells to generate positive MSR signals. This stimulatory effect was not influenced by the presence of MICA but was significantly enhanced ($p < 0.05$) by the concomitant presence of 4HNE (Fig. 6C). Dose-dependent studies demonstrated that the impact of BP was preferentially on MSR-detected mitochondrial ROS ($p < 0.001$), with >70% of live cells positive at the lowest dose tested (25 μM) compared with 40–50% when overall cellular ROS production was measured with DHE ($p < 0.05$) (Fig. 6D). BP also recapitulated the impact of 4HNE and acrolein on human spermatozoa in precipitating a highly significant decline of sperm motility ($p < 0.001$) in the absence of any change in cell vitality (Fig. 6E).

Because MICA did not enhance mitochondrial ROS generation, these results suggested that BP must be interacting with a mitochondrial target other than dihydrolipoyl dehydrogenase to cause such a dramatic change in mitochondrial free radical generation. A likely candidate in this regard is SDH, which has previously been found to be targeted by both BP (32) and 4HNE (33, 34). Accordingly, 4HNE was assessed for its ability to inhibit the activity of SDH and was found to be extremely active (supplemental Fig. 4). By contrast, treatment of the spermatozoa with 4HNE did not significantly reduce the activity of another frequently cited target for 4HNE adduction, cytochrome *c* oxidase (supplemental Fig. 4).

The particular ability of 4HNE to target SDH in sperm mitochondria was also confirmed using Western blotting and pull-down procedures. The initial analysis involved probing a Western blot of human spermatozoa with an antibody against SDHA, the 72-kDa catalytic subunit of SDH complex II of the mitochondrial electron transport chain. This study clearly revealed a protein of the anticipated molecular mass in human spermatozoa; furthermore, a cross-reactive 4HNE band was identified in exactly the same location when the blot was stripped and reprobed with an antibody against 4HNE (Fig. 7A). To be certain that the SDHA and 4HNE bands were one and the same protein, the SDHA protein was pulled down from a sperm lysate and the isolated protein probed with antibodies against SDHA and 4HNE. The results of this analysis clearly indicated that SDH is a major target for 4HNE adduction (Fig. 7B). The mechanism by which the adduction of SDHA leads to the activation of mitochondrial ROS does not seem to involve a change in the stability of this protein (Fig. 7C). Rather, the primary impact of 4HNE is to covalently bind SDHA disrupting the functionality of this molecule so that it auto-oxidizes and adventitiously transfers electrons to oxygen in the manner described by Messner and Imlay (35).

Further evidence for this conclusion came from an analysis of the influence DPI on ROS generation in response to 4HNE. DPI is a flavoprotein inhibitor, and SDHA is a flavoprotein. Accordingly, the addition of DPI (10 μM) led to a highly significant reduction ($p < 0.001$) in the redox response to 4HNE, as illustrated in Fig. 7D. It should also be noted that the addition of DPI enhanced the spontaneous ROS signal in these sperm populations, making it unlikely that NADPH oxidases such as NOX5

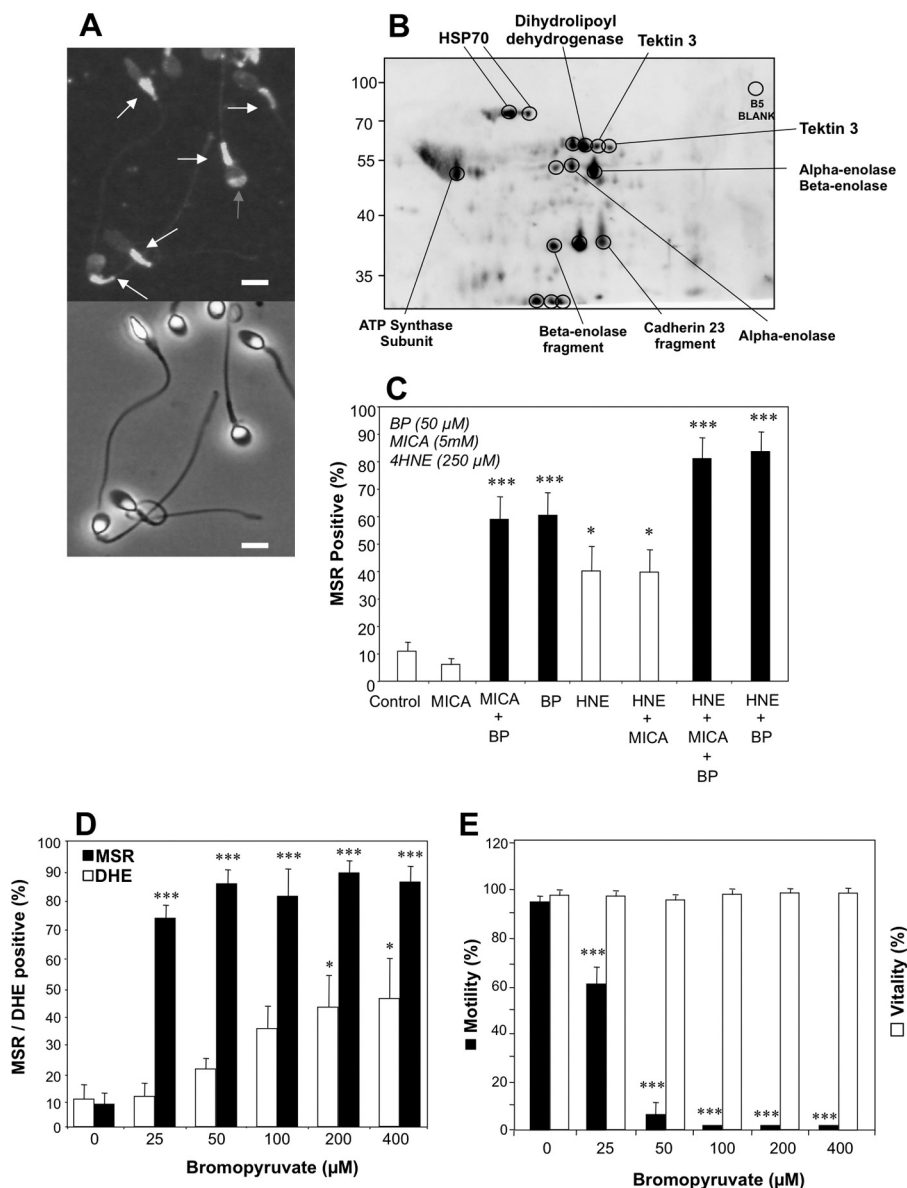


FIGURE 6. Identification of the site of 4HNE binding to human spermatozoa and characterization of the adducted proteins. *A*, using an anti-4HNE antibody it was possible to identify the sperm midpiece, where the sperm mitochondria are housed, as the major subcellular site of 4HNE binding (white arrows) although occasional signals were also detected in the sperm head (gray arrow). Lower panel represents the phase-contrast image of the antibody-stained cells. Scale bars, 5 μm. *B*, two-dimensional Western blot of the proteins adducted by 4HNE. Encircled spots were excised and submitted for proteomic analysis using a MALDI TOF/TOF mass spectrometer. Labels indicate the protein identifications secured in this analysis. *C*, analysis shows the ability of MICA and BP, alone and in combination with 4HNE (250 μM), to activate mitochondrial ROS generation in human spermatozoa. Filled bars highlight the stimulatory effect of BP. Data were analyzed by ANOVA, and values are presented as means ± S.E. (error bars); ***, $p < 0.001$; *, $p < 0.05$ for differences with vehicle control by Fisher's PLSD. Analyses were based on three independent semen samples. *D*, analysis shows the ability of BP to stimulate ROS generation in populations of human spermatozoa. Analyses of the general cellular ROS signal detected with DHE (open bars) and mitochondrial ROS monitored with MSR (filled bars) demonstrate the latter to be preferentially induced by BP. Data were analyzed by ANOVA, and values are presented as means ± S.E.; ***, $p < 0.001$; *, $p < 0.05$ for differences with vehicle control by Fisher's PLSD. Analyses were based on three independent semen samples. *E*, dose-dependent analysis of the impact of BP on motility (filled bars) and vitality of human spermatozoa (open bars) reveals a highly selective impact on the former. Data were analyzed by ANOVA, and the values are presented as means ± S.E.; ***, $p < 0.001$ for differences with vehicle control by Fisher's PLSD. Analyses were based on three independent semen samples.

are making a significant contribution to the basal levels of superoxide generation in these cells (Fig. 7D).

Finally, if the generation of electrophilic aldehydes during sperm metabolism is responsible for activating mitochondrial ROS production and initiating the intrinsic apoptotic cascade, then the addition of membrane-permeant nucleophiles should be able to arrest this process. To test this concept, the apoptotic process was seeded in populations of human spermatozoa by an

initial exposure to 100 μM 4HNE for 30 min. 4HNE was then washed out of the cell suspensions, and they were then incubated for 24 h at 37 °C in the presence or absence of a nucleophile in the form of penicillamine (0.125 and 0.250 mM). Electrophilic activation of the apoptotic cascade in these cells resulted in the anticipated loss of motility; however, this process was completely reversed by the presence of penicillamine (Fig. 7D).

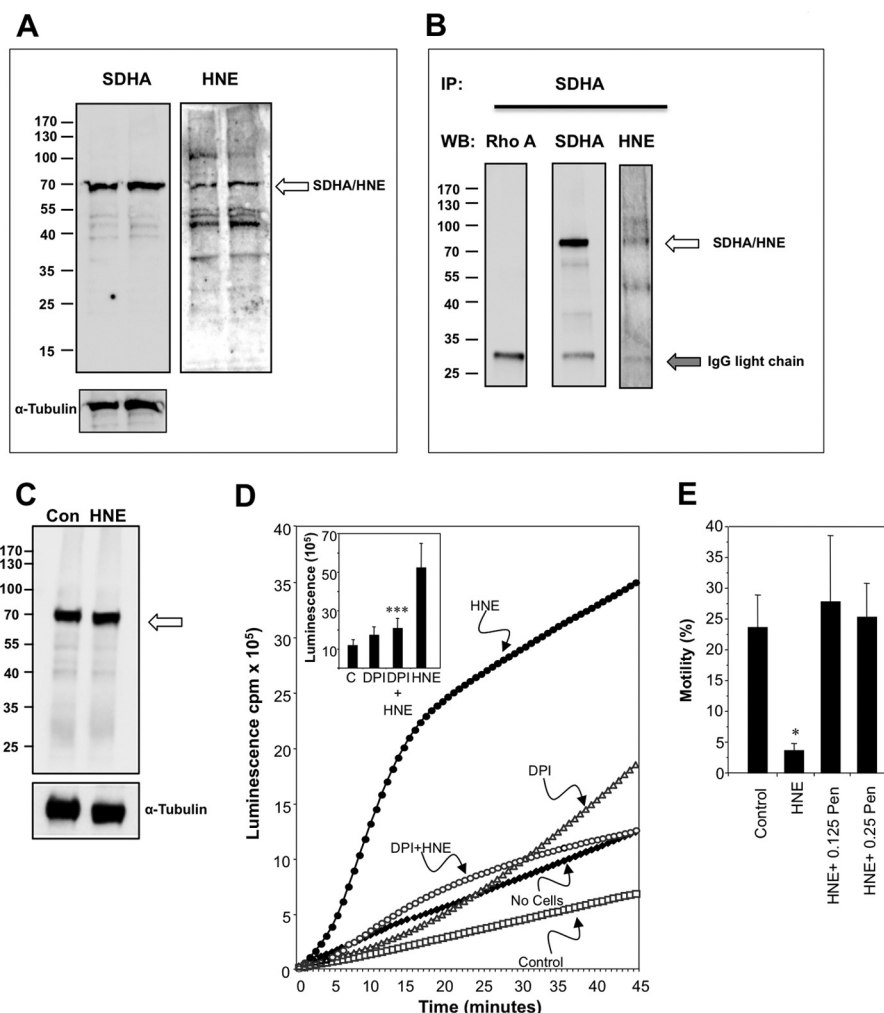


FIGURE 7. Evidence for the involvement of SDH in the mechanisms by which 4HNE triggers ROS generation by sperm mitochondria and the protective action of a nucleophile, penicillamine. *A*, Western blotting was used to analyze two independent samples for the presence of SDHA, the flavoprotein subunit of the SDH complex. When probed with an anti-SDHA antibody a clear single band was detected of the appropriate molecular mass. When this blot was stripped and reprobed with the anti-4HNE antibody, the same protein was clearly identified (arrowed) along with other 4HNE-positive proteins in the sperm lysate. *Inset*, α -tubulin loading controls. *B*, to focus the analysis on SDH, the latter was immunoprecipitated (IP) with the anti-SDHA antibody and the immunoprecipitate probed with antibodies against both SDHA and 4HNE. In the immunoprecipitate a band of the appropriate molecular mass was detected with both anti-SDHA and 4HNE antibodies as indicated by the arrow. A control Western blot (WB) was conducted using an irrelevant antibody (anti-Rho A). *C*, Western blot analysis confirmed that the induction of mitochondrial ROS with 4HNE (100 μ M) did not involve any change in the intracellular stability of SDH (arrowed). *D*, chemiluminescence analysis used a luminol/horseradish peroxidase system to detect extracellular H_2O_2 (5), revealed the ability of DPI (10 μ M), a flavoprotein inhibitor, to suppress the ROS response to 4HNE. *Inset* presents the integrated counts demonstrating the statistical significance of the suppression achieved with DPI. Data were analyzed by ANOVA, and values are presented as means \pm S.E. (error bars); ***, $p < 0.001$, for difference between 4HNE and 4HNE + DPI by Fisher's PLSD. Analyses were based on three independent semen samples. *E*, human spermatozoa were incubated for 24 h at 37 $^{\circ}$ C either untreated (Control) or after initiating apoptosis with a brief 30-min exposure to 100 μ M 4HNE. Following treatment the cells were centrifuged and resuspended in control medium BWB (4HNE) or medium supplemented with a nucleophile, penicillamine (Pen) at 0.125 and 0.25 mM. Treatment with 4HNE resulted in a significant loss of motility that was completely rescued by the concomitant presence of penicillamine. Data were analyzed by ANOVA, and values are presented as means \pm S.E.; *, $p < 0.05$ for differences with vehicle control by Fisher's PLSD. Analyses were based on four independent semen samples.

DISCUSSION

Oxidative stress is known to play a major role in the etiology of male infertility; however, the subcellular origins of the ROS responsible for this stress have been the subject of considerable uncertainty and some controversy (21, 36). Significant advances in this context have been: (i) the discovery that a major source of free radicals in defective human spermatozoa is the mitochondria (18, 37), (ii) that mitochondrial ROS generation is part of the intrinsic apoptotic cascade to which these cells default as a form of programmed senescence (22), and (iii) that the mechanisms responsible for ROS generation are self-perpetuating in that exposure to oxidants stimulates yet more

ROS production by these cells (19). In this study we have investigated the causative mechanisms that underpin these observations and, in the process, generated information that may be helpful in developing strategies to manage oxidative stress in the male germ line.

It has been recognized for some time that spermatozoa are very susceptible to lipid peroxidation because they are heavily endowed with polyunsaturated fatty acids (8). Moreover, the greater the polyunsaturated fatty acid content of these cells, the higher the levels of ROS generation by their mitochondria (37). In this study we have demonstrated that the spontaneous level of ROS generation by human sperm mitochondria is highly

correlated with the levels of lipid peroxide, measured as 4HNE, being generated by these cells ($R^2 = 0.89$). The causative nature of this relationship was suggested by the fact that a diverse array of natural and synthetic electrophiles were found to be powerful inducers of mitochondrial ROS generation in human spermatozoa. Furthermore, in the case of 4HNE, the stimulation of mitochondrial ROS production and concomitant motility loss were observed with doses of this compound that were within the physiological range. Thus, when cells are oxidatively stressed, the cellular concentrations of 4HNE are held to range between 10 μM and 5 mM (29, 38) whereas our study demonstrated significant effects of this electrophile at doses between 6.25 and 400 μM . The ability of individual electrophiles to stimulate mitochondrial ROS correlated reasonably well with measurements of their capacity to adduct the model nucleophile, reduced glutathione. By contrast, theoretical calculations of the corresponding electron reduction potentials showed very little correlation with the ROS-generating activity of these compounds, presumably because such assessments do not take into account the characteristics of the reacting nucleophiles. In a biological context, the fact that spermatozoa possess an array of proteins with reactive nucleophilic centers means that the targets for these electrophilic lipid aldehydes will be extremely complex, as revealed by the Western blot images presented in Fig. 6B.

The ability of lipid aldehydes to stimulate ROS generation by Michael addition reactions with mitochondrial proteins has been observed in other cell types and would clearly account for the oxidant-induced ROS generation cycle observed in human spermatozoa (19, 39). In terms of the specific mitochondrial protein responsible for ROS production, this study ruled out cytochrome oxidase as a candidate, even though 4HNE adduction of this molecule has been associated with mitochondrial ROS generation in other cell types (40). We were also able to rule out mitochondrial ATPase and the pyruvate dehydrogenase complex as being causally involved in the activation of ROS generation even though both of these complexes were clearly targeted by 4HNE and the latter has been identified as a source of mitochondrial ROS in other cells (41). Rather, the adducted molecule responsible for mitochondrial ROS generation in spermatozoa appeared to be the flavoprotein component of SDH. Thus, bromopyruvate, a known inhibitor of SDHA, efficiently activated mitochondrial ROS generation in these cells. Furthermore, Western blot analyses involving whole cell lysates and immunoprecipitated SDH demonstrated the latter to be a major 4HNE-adducted sperm protein. In addition, the ability of the flavoprotein inhibitor DPI to suppress 4HNE-induced mitochondrial ROS generation by human spermatozoa is consistent with the involvement of SDHA (which contains a covalently attached flavin adenine dinucleotide cofactor) in this process. Direct measurements of SDH activity in human spermatozoa also confirmed the ability of 4HNE to suppress this enzyme in a dose-dependent manner. The central involvement of SDH is also in keeping with the apparent importance of succinate in regulating mitochondrial ROS in other cell types (42) and the fact that isolated SDH is reportedly capable of generating superoxide anion (43). It also accords with a report by Lashin *et al.* (34) highlighting the importance of SDH as a target

for 4HNE in the pathogenesis of diabetic cardiomyopathy. It is therefore possible that SDH has general significance as a target for the lipid peroxides generated as a consequence of cell metabolism with subsequent activation of mitochondrial ROS and apoptosis, resulting in pathological changes in the affected cells. However, at this stage, we cannot absolutely rule out some contribution from other flavoproteins, including NADPH oxidases such as NOX5, to the 4HNE-induced ROS signal in human spermatozoa.

The ability of cytotoxic aldehydes generated as the result of oxidative stress to activate mitochondrial ROS production, directs human spermatozoa down a pathway of programmed senescence that has many of the hallmarks of the conventional intrinsic apoptotic cascade, as well as some distinct differences, largely due to the highly compartmentalized physical architecture of these cells (22). As a consequence of activating this apoptotic cascade mitochondrial ROS trigger a rapid loss of mitochondrial membrane potential and motility followed, much later, by caspase activation, phosphatidylserine exteriorization, and high levels of lipid peroxidation. Later still, we see evidence of oxidative DNA damage and strand breakage in concert with a profound loss of cell viability. This cascade of events, triggered by the adduction of mitochondrial SDH by lipid peroxides and culminating in cell death and DNA damage, precisely mirrors the phenotype of spermatozoa from infertile men which have been shown to feature a loss of mitochondrial membrane potential, reduced motility, enhanced mitochondrial ROS generation, oxidative DNA damage, DNA fragmentation, and high levels of cell death (10, 18, 23, 44, 45). In light of these observations, it may be possible to extend the life span of mammalian spermatozoa *in vitro* by incorporating nucleophiles into the incubation medium to intercept lipid peroxides as they are generated, thereby preventing them from gaining access to the mitochondrial electron transport chain and activating the apoptotic cascade described in this paper. The positive results obtained with penicillamine in this study suggest that such an approach may have some practical merit.

Acknowledgments—We thank Jodi Powell for organizing our panel of normal semen donors and Haley Connaughton for technical assistance.

REFERENCES

- Dohle, G. R., Colpi, G. M., Hargreave, T. B., Papp, G. K., Jungwirth, A., and Weidner, W. (2005) EAU guidelines on male infertility. *Eur. Urol.* **48**, 703–711
- Hull, M. G., Glazener, C. M., Kelly, N. J., Conway, D. I., Foster, P. A., Hinton, R. A., Coulson, C., Lambert, P. A., Watt, E. M., and Desai, K. M. (1985) Population study of causes, treatment, and outcome of infertility. *BMJ* **291**, 1693–1697
- Aitken, R. J., and Clarkson, J. S. (1987) Cellular basis of defective sperm function and its association with the genesis of reactive oxygen species by human spermatozoa. *J. Reprod. Fertil.* **81**, 459–469
- Alvarez, J. G., Touchstone, J. C., Blasco, L., and Storey, B. T. (1987) Spontaneous lipid peroxidation and production of hydrogen peroxide and superoxide in human spermatozoa: superoxide dismutase as major enzyme protectant against oxygen toxicity. *J. Androl.* **8**, 338–348
- Aitken, R. J., Irvine, D. S., and Wu, F. C. (1991) Prospective analysis of sperm-oocyte fusion and reactive oxygen species generation as criteria for the diagnosis of infertility. *Am. J. Obstet. Gynec.* **164**, 542–551

6. Aitken, R. J., Clarkson, J. S., and Fishel, S. (1989) Generation of reactive oxygen species, lipid peroxidation, and human sperm function. *Biol. Reprod.* **41**, 183–197
7. Aitken, J., and Fisher, H. (1994) Reactive oxygen species generation and human spermatozoa: the balance of benefit and risk. *Bioessays* **16**, 259–267
8. Jones, R., Mann, T., and Sherins, R. (1979) Peroxidative breakdown of phospholipids in human spermatozoa, spermicidal properties of fatty acid peroxides, and protective action of seminal plasma. *Fertil. Steril.* **31**, 531–537
9. De Iuliis, G. N., Thomson, L. K., Mitchell, L. A., Finnie, J. M., Koppers, A. J., Hedges, A., Nixon, B., and Aitken, R. J. (2009) DNA damage in human spermatozoa is highly correlated with the efficiency of chromatin remodeling and the formation of 8-hydroxy-2'-deoxyguanosine, a marker of oxidative stress. *Biol. Reprod.* **81**, 517–524
10. Aitken, R. J., and De Iuliis, G. N. (2010) On the possible origins of DNA damage in human spermatozoa. *Mol. Hum. Reprod.* **16**, 3–13
11. Aitken, R. J., and Curry, B. J. (2011) Redox regulation of human sperm function: from the physiological control of sperm capacitation to the etiology of infertility and DNA damage in the germ line. *Antioxid. Redox Signal.* **14**, 367–381
12. Totic, J., and Walton, A. (1946) Formation of hydrogen peroxide by spermatozoa and its inhibitory effect of respiration. *Nature* **158**, 485
13. de Lamirande, E., and Gagnon, C. (1993) Human sperm hyperactivation and capacitation as parts of an oxidative process. *Free Rad. Biol. Med.* **14**, 157–166
14. Bize, I., Santander, G., Cabello, P., Driscoll, D., and Sharpe, C. (1991) Hydrogen peroxide is involved in hamster sperm capacitation *in vitro*. *Biol. Reprod.* **44**, 398–403
15. Aitken, R. J., Harkiss, D., Knox, W., Paterson, M., and Irvine, D. S. (1998) A novel signal transduction cascade in capacitating human spermatozoa characterised by a redox-regulated, cAMP-mediated induction of tyrosine phosphorylation. *J. Cell Sci.* **111**, 645–656
16. Zini, A., and Sigman, M. (2009) Are tests of sperm DNA damage clinically useful? Pros and cons. *J. Androl.* **30**, 219–229
17. Storey, B. T. (2008) Mammalian sperm metabolism: oxygen and sugar, friend and foe. *Int. J. Dev. Biol.* **52**, 427–437
18. Koppers, A. J., De Iuliis, G. N., Finnie, J. M., McLaughlin, E. A., and Aitken, R. J. (2008) Significance of mitochondrial reactive oxygen species in the generation of oxidative stress in spermatozoa. *J. Clin. Endocrinol. Metab.* **93**, 3199–3207
19. du Plessis, S. S., McAllister, D. A., Luu, A., Savia, J., Agarwal, A., and Lampiao, F. (2010) Effects of H₂O₂ exposure on human sperm motility parameters, reactive oxygen species levels and nitric oxide levels. *Andrologia* **42**, 206–210
20. Biggers, J. D., Whitten, W. K., and Whittingham, D. G. (1997) in *Methods in Mammalian Embryology* (Daniel, J. C., ed) pp. 86–116, Freeman, San Francisco
21. Aitken, R. J., Ryan, A. L., Curry, B. J., and Baker, M. A. (2003) Multiple forms of redox activity in populations of human spermatozoa. *Mol. Hum. Reprod.* **9**, 645–661
22. Koppers, A. J., Mitchell, L. A., Wang, P., Lin, M., and Aitken, R. J. (2011) Phosphoinositide 3-kinase signalling pathway involvement in a truncated apoptotic cascade associated with motility loss and oxidative DNA damage in human spermatozoa. *Biochem. J.* **436**, 687–698
23. Mitchell, L. A., De Iuliis, G. N., and Aitken, R. J. (2011) The TUNEL assay consistently underestimates DNA damage in human spermatozoa and is influenced by DNA compaction and cell vitality: development of an improved methodology. *Int. J. Androl.* **34**, 2–13
24. Baker, M. A., Lane, D. J., Ly, J. D., De Pinto, V., and Lawen, A. (2004) VDAC1 is a transplasma membrane NADH-ferricyanide reductase. *J. Biol. Chem.* **279**, 4811–4819
25. Hutson, S. M., Van Dop, C., and Lardy, H. A. (1977) Mitochondrial metabolism of pyruvate in bovine spermatozoa. *J. Biol. Chem.* **252**, 1309–1315
26. Parr, R. G., Szentpaly, L. V., and Liu, S. (1999) Electrophilicity index. *J. Am. Chem. Soc.* **121**, 1922–1924
27. Böhme, A., Thaens, D., Paschke, A., and Schüürmann, G. (2009) Kinetic glutathione chemoassay to quantify thiol reactivity of organic electrophiles: application to α,β -unsaturated ketones, acrylates, and propiolates. *Chem. Res. Toxicol.* **22**, 742–750
28. Hughes, L. M., Griffith, R., Carey, A., Butler, T., Donne, S. W., Beagley, K. W., and Aitken R. J. (2009) The spermstatic and microbicidal actions of quinones and maleimides: toward a dual-purpose contraceptive agent. *Mol. Pharmacol.* **76**, 113–124
29. Uchida K. (2003) 4-Hydroxy-2-nonenal: a product and mediator of oxidative stress. *Prog. Lipid Res.* **42**, 318–343
30. Kumar, V., Kota, V., and Shivaji, S. (2008) Hamster sperm capacitation: role of pyruvate dehydrogenase A and dihydrolipoamide dehydrogenase. *Biol. Reprod.* **79**, 190–199
31. Maldonado, M. E., Oh, K. J., and Frey, P. A. (1972) Studies on *Escherichia coli* pyruvate dehydrogenase complex. I. Effect of bromopyruvate on the catalytic activities of the complex. *J. Biol. Chem.* **247**, 2711–2716
32. Sanborn, B. M., Felberg, N. T., and Hollocher, T. C. (1971) The inactivation of succinate dehydrogenase by bromopyruvate. *Biochim. Biophys. Acta* **227**, 219–231
33. Picklo, M. J., Amarnath, V., McIntyre, J. O., Graham, D. G., and Montine, T. J. (1999) 4-Hydroxy-2(E)-nonenal inhibits CNS mitochondrial respiration at multiple sites. *J. Neurochem.* **72**, 1617–1624
34. Lashin, O. M., Szveda, P. A., Szveda, L. I., and Romani, A. M. (2006) Decreased complex II respiration and HNE-modified SDH subunit in diabetic heart. *Free Radic. Biol. Med.* **40**, 886–896
35. Messner, K. R., and Imlay, J. A. (2002) Mechanism of superoxide and hydrogen peroxide formation by fumarate reductase, succinate dehydrogenase, and aspartate oxidase. *J. Biol. Chem.* **277**, 42563–42571
36. Ford, W. C. (2004) Regulation of sperm function by reactive oxygen species. *Hum. Reprod. Update* **10**, 387–399
37. Koppers, A. J., Garg, M. L., and Aitken, R. J. (2010) Stimulation of mitochondrial reactive oxygen species production by unesterified, unsaturated fatty acids in defective human spermatozoa. *Free Radic. Biol. Med.* **48**, 112–119
38. Chen, Z. H., and Niki, E. (2006) 4-Hydroxynonenal (4-HNE) has been widely accepted as an inducer of oxidative stress: is this the whole truth about it or can 4-HNE also exert protective effects? *IUBMB Life* **58**, 372–373
39. Landar, A., Zmijewski, J. W., Dickinson, D. A., Le Goffe, C., Johnson, M. S., Milne, G. L., Zannoni, G., Vidari, G., Morrow, J. D., and Darley-Usmar, V. M. (2006) Interaction of electrophilic lipid oxidation products with mitochondria in endothelial cells and formation of reactive oxygen species. *Am. J. Physiol. Heart Circ. Physiol.* **290**, H1777–1787
40. Chen, J., Henderson, G. I., and Freeman, G. L. (2001) Role of 4-hydroxynonenal in modification of cytochrome c oxidase in ischemia/reperfusion rat heart. *J. Mol. Cell Cardiol.* **33**, 1919–1927
41. Bunik, V. I., and Sievers, C. (2002) Inactivation of the 2-oxo acid dehydrogenase complexes upon generation of intrinsic radical species. *Eur. J. Biochem.* **269**, 5004–5015
42. Zoccarato, F., Cavallini, L., and Alexandre, A. (2009) Succinate is the controller of O₂-/H₂O₂ release at mitochondrial complex I: negative modulation by malate, positive by cyanide. *J. Bioenerg. Biomembr.* **41**, 387–393
43. Zhang, L., Yu, L., and Yu, C. A. (1998) Generation of superoxide anion by succinate-cytochrome c reductase from bovine heart mitochondria. *J. Biol. Chem.* **273**, 33972–33976
44. Espinoza, J. A., Schulz, M. A., Sánchez, R., and Villegas, J. V. (2009) Integrity of mitochondrial membrane potential reflects human sperm quality. *Andrologia* **41**, 51–54
45. Aitken, R. J., Findlay, J. K., Hutt, K. J., and Kerr, J. B. (2011) Apoptosis in the germ line. *Reproduction* **141**, 139–150